Journal of Analytical and Applied Pyrolysis 150 (2020) 104866

Contents lists available at ScienceDirect

Journal of Analytical and Applied Pyrolysis

journal homepage: www.elsevier.com/locate/jaap

Treatment of high-ash industrial sludge for producing improved char with low heavy metal toxicity

Shengyu Xie[a,b], Guangwei Yu[a,*], Chunxing Li[c], Jie Li[a], Gang Wang[a], Shaoqing Dai[a], Yin Wang[a]

[a] CAS Key Laboratory of Urban Pollutant Conversion, Institute of Urban Environment, Chinese Academy of Sciences, 1799 Jimei Road, Xiamen 361021, China
[b] Graduate School of Environmental Studies, Tohoku University, 6-6-07 Aoba, Aramaki-aza, Aoba-ku, Sendai, Miyagi 980-8579, Japan
[c] Department of Environmental Engineering, Technical University of Denmark, Kgs. Lyngby DK-2800, Denmark

ARTICLE INFO

Keywords:
Industrial sludge
Rice straw
Co-pyrolysis
Char property
Heavy metal

ABSTRACT

Industrial sludge is a type of solid waste that is known for its high ash content and heavy metal concentrations. In this study, industrial sludge was used for co-pyrolysis with rice straw at different temperatures (400, 500, and 600 °C) and mixture proportions (1:0, 9:1, 4:1, and 3:2, w/w). The relationship between heavy metal speciation and char properties was characterized in detail to investigate the effects of co-pyrolysis. Results show that the addition of rice straw can decrease the ash content and increase thermal stability and pore structure of char due to its high organic content. Simultaneously, co-pyrolysis decreases heavy metal concentrations and enhances the transformation of Cr, Zn, and Cd to a more stable fraction, with higher alkalinity, aromaticity, and specific surface area of char. Moreover, the leaching toxicity of Zn with high content is decreased to below threshold values, and the potential ecological risk of char is reduced to the lowest level under the condition of 600 °C with a mixing proportion of 4:1. This work demonstrates that co-pyrolysis provides an effective industrial sludge treatment for improving char characteristics and immobilizing heavy metals, indicating its superior application potential.

1. Introduction

Industrial sludge (IS) is a byproduct of processes from steel, electroplating, paper mill, and chemical industry wastewater treatment. It has engendered serious environmental concern over the past few decades owing to rapid industrialization [1]. According to the China Environment Statistical Yearbook (2017), approximately 37.78 billion kilograms of IS (80 % moisture content) are produced in China. IS has high ash content and is rich in some metallic oxides such as silicon, iron, and aluminum, along with abundant pathogens, microorganisms, and organic pollutants [2]. Furthermore, the properties of heavy metals (HMs) in IS are closely related to their origin. For example, the Cr concentration in tannery sludge exceeds 5000 mg/kg, and Ni is the main hazardous element in sludge from metal and battery fields [1]. Without proper treatment, these HMs in IS accumulate in the human body through food chain [3]. At present, landfill, incineration, and agricultural application are still the common methods for sludge treatment [4]; however, some characteristics of sludge such as high ash content, organic pollutants, and HMs risk limit the agricultural application of traditional technologies [5].

Pyrolysis has presented some advantages for sludge treatment in recent years. It can effectively reduce sludge volume and eliminate pollutants [6] and simultaneously, some bio-available HMs are transformed to more stable fractions at high temperatures [7]. Conversely, the char obtained can be used for satisfactory adsorption and soil remediation because of its pore structure, abundant functional groups, and plentiful nutrients elements [8,9]. The pure pyrolysis of sludge still has some deficiencies such as low energy utilization efficiency and poor char properties [10] and therefore, other types of solid waste have been widely used in the formation of char. For example, the addition of corncob with increased temperatures is beneficial to the production of H_2 and organic acids, with a high heating value during the pyrolysis of sludge [11]. The co-pyrolysis of municipal sludge and rice husk can capture more gaseous hydrocarbons and promote the carbonization and aromatization of char [12]. Yin et al. [13] verified that the sludge char obtained at 600 °C, with the addition of 25 % walnut shell, exhibited a high specific surface area of 47.13 m^2/g. The maximum adsorption capacity of NH_4^+ reached 22.85 mg/g after the formation of additional

Abbreviations: IS, industrial sludge; HM, heavy metal; RS, rice straw; TGA, thermogravimetric analysis; BET, Brunauer–Emmett–Teller; BCR, European Community Bureau of Reference; TCLP, toxicity characteristic leaching procedure

* Corresponding author.
E-mail address: gwyu@iue.ac.cn (G. Yu).

https://doi.org/10.1016/j.jaap.2020.104866
Received 24 April 2020; Received in revised form 3 June 2020; Accepted 8 June 2020
Available online 13 June 2020

adsorption active sites. The co-pyrolysis of municipal sludge and bamboo sawdust led to a 50 % reduction in HM concentrations (Cu, Zn, Pb, Cr, Mn, and Ni) of char, and the speciation of HMs was transferred from the exchangeable and reducible fractions to the residual fraction [14]. This was because the solute HMs were entrapped or chelated with some functional groups for further immobilization during treatment. Moreover, pyrolysis technology has been widely used for HM immobilization in the treatment of sludge from paper mills, electronic industrial applications, and the textile dyeing process [15–17]. Chanaka Udayanga et al. [18] also found that pyrolysis treatment at 400–600 °C could effectively enhance the immobilization of HMs in IS. The formation of metal halides at higher temperatures would cause an increase in the leaching toxicity of Mn, Cu, and Zn. However, the effects of biomass on HMs toxicity during IS pyrolysis need to be further verified.

The production of rice straw (RS) is approximately 200 billion kilograms annually in China, and its direct discard and combustion leads to serious air pollution [19]. The high content of lignocellulose and low amount of silica make RS an excellent pyrolysis material [20]. Therefore, the co-pyrolysis of sludge and RS can achieve the synergistic disposal and utilization of wastes. Consequently, pyrolysis behavior and char characteristics have been studied in traditional and microwave technology [20–22]. However, there is little information regarding the migration and transformation of HMs during the co-pyrolysis of RS and sludge, especially for IS with high contents and risk of HMs. Further research is necessary to explore how the improvement in char properties affects the immobilization of HMs during IS pyrolysis with the addition of RS.

The main objectives of the present study are to: (1) comprehensively investigate the properties of char from co-pyrolysis such as chemical composition, micromorphology, and functional groups; (2) study the conversion of HM speciation and the potential ecological risk of char; and (3) explore the interactions between char improvement and HMs immobilization.

2. Materials and methods

2.1. Raw materials

The naturally dry IS was sampled from a chemical fiber industrial wastewater treatment plant in Jilin City, China, based on an anoxic–oxic (A/O) process. The used RS in the experiment was collected from a farm in Xiamen City, China. The IS and RS were added in a drying oven for 24 h at 105 °C. The dried materials were ground, sieved (less than 0.15 mm), and kept in a glass desiccator for subsequent experiments. The basic properties of the IS and RS are listed in **Table S1**.

2.2. Pyrolysis experiments

Char samples were prepared by a fixed-bed pyrolysis reactor (**Fig. S1a**). Details of the apparatus have been previously reported [23]. In the current experiment, a 40 g homogenous mixing sample, prepared with IS:RS ratios (on dry weight basis) of 1:0, 9:1, 4:1, and 3:2 was loaded into a quartz tube located in the center of the pyrolysis apparatus. To create an anaerobic environment, nitrogen of 80 mL/min was then used to remove the air in the quartz tube. The pyrolysis apparatus was then heated to a pre-set temperature (400, 500, or 600 °C) from ambient temperature at a heating rate of 10 °C /min, respectively. After maintaining the system at the target temperature for 60 min, heating was stopped, and the quartz tube was cooled to 30 °C with continued nitrogen flow. All the char samples obtained were stored in a glass desiccator for subsequent analysis after the char yield was calculated and named S4R1 − 400, S4R1 − 500, S1R0 − 600, S9R1 − 600, S4R1 − 600, and S3R2 − 600, based on the IS:RS ratio and the pre-set temperature.

2.3. Characterization analysis

Thermogravimetric analysis (TGA) was performed (TGA 209 F3, Netzsch, Germany) for 10 mg of raw material with a temperature ranging from 40 to 900 °C under a heating rate of 10 °C/min with the carrier gas (nitrogen) of 60 mL/min and protective gas (nitrogen) of 20 mL/min, respectively. The pH of the solid sample was measured by a pH meter after extraction using deionized water at a ratio of 1:20 (w/v) [16]. Proximate analysis was conducted via combustion according to the Chinese National Standard (GB/T 28731 − 2012). Elemental analysis was performed with an elemental analyzer (VarioEL III, Germany) via combustion at 950 °C. The specific surface area, pore volume, and average pore diameter were calculated according to the Brunauer–-Emmett–Teller (BET) method after obtaining the 77.4 K nitrogen adsorption/desorption isotherms with a Tristar 3000 analyzer (Tristar 3000, USA) and the calculated methods referred to in other research [24]. The micromorphology was characterized by scanning electron microscopy (S-4800, Hitachi, Japan) with an accelerating voltage of 5.00 kV. The surface functional groups were examined by fourier transform infrared spectrometry (iS10, Thermo, USA) after the dried samples were mixed with KBr at 1:100. The main ash-forming components were measured using X-ray fluorescence (XRF, Axios-MAX, Netherlands) after the sample was compressed into tablet. The phase composition of the sample was analyzed via X-ray diffraction (X' Pert Pro, PANalytical B. V.) and the relevant tests referred to standard power diffraction procedures [25].

2.4. Heavy metals analysis

The speciation distributions of HMs in the samples were analyzed according to the three-step extraction procedure from the European Community Bureau of Reference (BCR), which are classified as exchangeable fraction (F1), reducible fraction (F2), oxidizable fraction (F3), and residual fraction (F4). The extraction of the total HMs was referred to the F4 procedure (**Fig. S1b**) [26]. The leaching toxicity of HMs was analyzed by taking the solution (sample to acetic acid ratio of 1:20) and shaking it for 18 h at 200 r/min, adhering to the toxicity characteristic leaching procedure (TCLP) [16]. The extracted solutions were tested with an inductively coupled plasma mass spectrometry (Agilent 7500, USA) after centrifugation, filtration, and constant-volume.

The residual rate (R, %) was used to show the enrichment degree of HM in char, with the following calculation:

$$R = \frac{C_c}{XC_r + (100 - X)C_s} \times Y \times 100 \quad (1)$$

where C_c (mg/kg) is the total concentration of each HM in char; C_r and C_s (mg/kg) are the total concentrations of the individual HM in RS and IS, respectively; X (%) is the proportion of RS addition; Y (%) is the yield of char after pyrolysis.

The environmental impact of HMs in the sample can be assessed by the potential ecological risk, which was calculated as follows [16]:

$$C_f = C_i / C_n \quad (2)$$

$$E_r = T_r \times C_f \quad (3)$$

$$RI = \Sigma E_r \quad (4)$$

where C_f is the individual HM contamination; C_i presents the F1 + F2 + F3 fractions; C_n presents the F4 fraction; T_r is the individual HM toxicity response factor with the following values, Cd (30), Ni (6), Cu (5), Pb (5), Cr (2), and Zn (1); E_r is the potential ecological risk index of an individual HM; RI is the potential ecological index of IS or char.

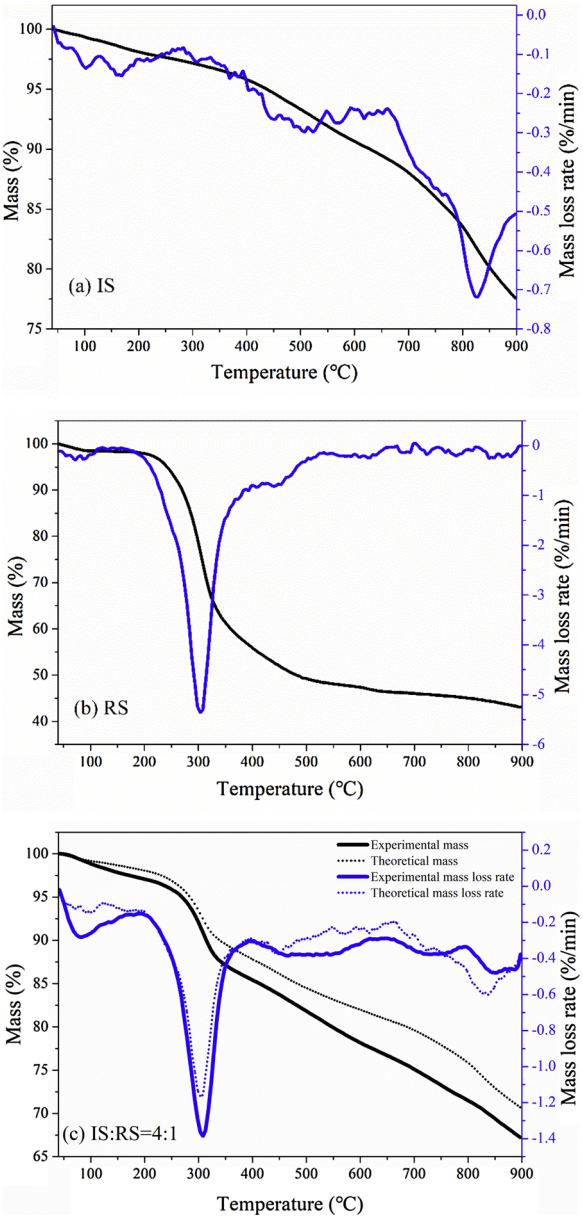

Fig. 1. Mass loss and mass loss rate curves of (a) industrials sludge, (b) rice straw, and (c) their mixture.

3. Results and discussion

3.1. Thermogravimetric analysis

The RS is significantly decomposed at 900 °C with a mass loss of 56.9 %, compared with an IS mass loss of 22.4 % (Fig. 1a–b). The differences in mass loss between IS and RS are attributed to the higher content of easily decomposed volatile matter in RS [27]. Simultaneously, the high residue mass after TGA of IS is related to its ash content (80.1 wt.%). For IS, the first decomposition stage extends from 87 °C to 237 °C, comprising the removal of bound water and lighter compounds [28]. The second stage of mass loss between 432 °C and 647 °C is due to the decomposition of higher molecular weight organic compounds [29]. Additionally, the main chemical conversion occurs in the temperature range of 800–850 °C, with the highest rate of 0.72 %/min at 828 °C, resulting from the decomposition of calcium carbonate and other minerals [30]. However, RS is converted in the temperature range of 200–550 °C, with the highest mass loss rate of 5.36 %/min at 303 °C. This phenomenon can be attributed to the decomposition and devolatilization of lignocellulose in biomass [31]. Conversely, the lack of evident peak in this temperature range is because of the low content of volatile substances in IS. Additionally, the synergistic effect of co-pyrolysis was studied by comparing the differences of experimental and theoretical data based on TGA (Fig. 1c). The accelerative co-pyrolysis interaction between 263–708 °C can be attributed to the large amount of Fe_2O_3, Al_2O_3, and SiO_2 in IS that acts as a catalyst to promote the decomposition of biomass tar [32]. The inhibitive effect occurred at 778–848 °C, suggesting that the more stable minerals are formed after co-pyrolysis. The additional mass loss after TGA, compared with theoretical data, suggests that co-pyrolysis can produce more oil and gas.

3.2. General properties of char

The physicochemical properties of char, including the yield, pH, proximate analysis, and elemental analysis, are summarized in Table 1. The yield of char decreases with rising pyrolysis temperature and RS proportion, which suggests that more volatile matter is released as oil and gas. Additionally, the more high-value products can be applied in a co-pyrolysis system for energy supplementary to reduce energy input and carbon emission [33]. The results are also verified in the mass and mass loss rate curves of raw materials (Fig. 1). The pH of char increases from 6.7 to 8.9 with increasing temperature, which is because all metal oxides and minerals are maintained in char after the decomposition of acidic functional groups, and the condensation of aliphatic substances [34,35]. The char obtained with alkalinity can be used as remediation in acid-contaminated soil [9,36]. In addition, pH was reported to have played an important factor in HM immobilization [37].

Table 1
Physicochemical properties of feedstocks and char samples.

Sample	Yield (%)	pH	Proximate analysis (wt. %)				Elementals analysis (wt. %)				
			Ash	VM[a]	FC[b]	C	H	N	S	H/C	N/C
IS	/	6.7	80.1	18.1	1.8	11.5	1.1	3.0	1.9	1.10	0.22
RS	/	7.7	17.0	66.6	16.4	34.0	5.1	1.4	0.1	1.80	0.04
S4R1－400	81.2	7.5	80.9	9.4	9.7	14.9	0.8	2.3	1.9	0.68	0.13
S4R1－500	80.4	8.4	84.1	5.6	10.3	15.1	0.7	2.0	2.0	0.53	0.11
S1R0－600	83.6	8.4	92.3	1.2	6.5	9.5	0.4	1.5	2.2	0.56	0.13
S9R1－600	79.3	8.6	90.7	1.4	7.9	12.8	0.5	1.4	2.2	0.46	0.09
S4R1－600	75.1	8.9	89.5	2.8	7.7	15.8	0. 6	1.3	2.1	0.42	0.07
S3R2－600	65.8	8.9	87.3	5.0	7.7	23.0	0.7	1.2	1.8	0.37	0.04

[a] VM, Volatile matter.
[b] FC, Fixed carbon.

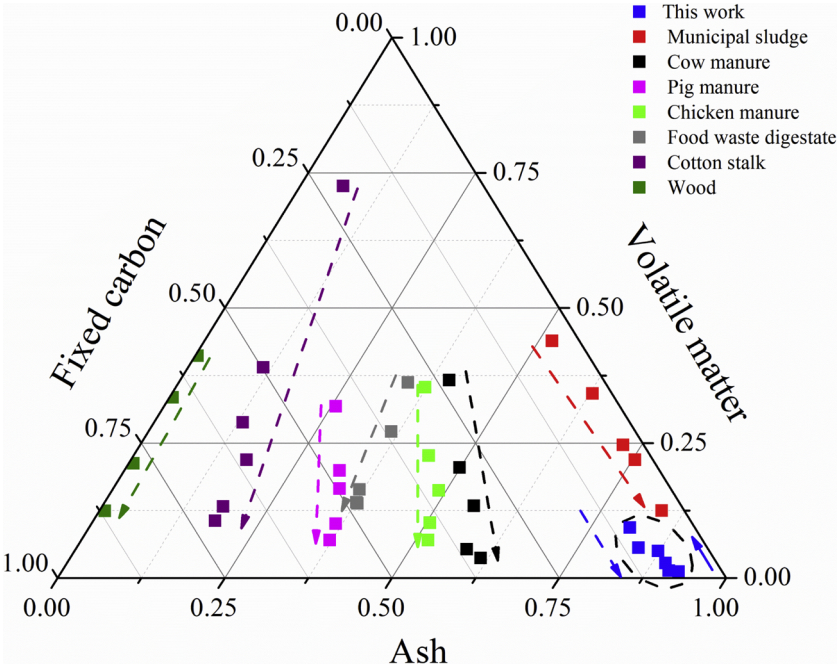

Fig. 2. Triangle plot of proximate analysis results for char (dash arrows show the trend with rising pyrolysis temperature and solid arrow indicates the trend with rising rice straw proportion).

The proximate analysis results show that RS has a higher volatile matter content (66.6 %) compared with 18.1 % for IS. The ash content of IS reaches 80.1 % owing to the high inorganic mineral content. The ash content increases markedly with increasing pyrolysis temperature as the variation affects the pH of char, as reported in other studies [35,37]. In particular, the high ash content of char (92.3 % at 600 °C) limits its further utilization. The ash content of char decreases, and the volatile matter content increases, after the addition of RS. Moreover, the content of fixed carbon is also increased in char compared with IS, suggesting higher thermal stability [28]. The triangle plot (Fig. 2) shows the proximate analysis data of different char samples obtained at 300–700 °C from municipal sludge [21], cow manure [38], pig manure [39], chicken manure [39], food waste digestate [40], cotton stalk [41], and wood [42]. The dashed arrows show the trend with rising pyrolysis temperature. For all materials, the rising pyrolysis temperature causes an increase in ash content and a decrease in volatile content in char. Higher ash and lower fixed carbon contents exist in sludge char compared with other char samples obtained by manure, digestate, and biomass, suggesting its limitation as a fuel [28]. Furthermore, the char from IS pyrolysis presents more ash and less volatiles than the municipal sludge char, suggesting its suitability for ceramsite material [43]. The addition of RS can improve the char properties and thermal stability (opposite trend to that of rising temperature) due to its high organic contents (Fig. 2).

The decreases in H and N contents after co-pyrolysis are attributed to the loss of volatile matter [34]. However, the contents of C and H increase significantly with the proportion of RS because of the high volatile matter in raw RS. Moreover, the variation in S content in char samples shows the opposite trend compared with those in C and H. The molar ratio of H/C declines markedly with an increase in pyrolysis temperature and RS proportion. The lower molar ratio of H/C indicates the occurrence of dehydrogenative polymerization and higher aromaticity of char [21,34]. The molar N/C ratio declines significantly with increasing pyrolysis temperature and RS proportion, which suggests the reduction of the N-related functional groups on the surface of the char [44]. Similar results have been observed in the pyrolysis of municipal sludge [14].

3.3. Surface morphology and porosity

The variations in the surface morphology of the samples after pyrolysis are shown in Fig. 3. There are many dense blocks relative to the inorganic condensed phase in IS and smooth lamellae in RS, indicating that the feedstocks have an undeveloped pore structure. These dense blocks in IS are broken up into small lumps after co-pyrolysis and the number of pores on the surfaces of the char samples increases significantly with an increase in temperature. Furthermore, adding RS has a positive effect on the formation of loose and developed surface morphology. This is because the gases produced by the thorough decomposition of organic matter can extend the pore structure of char at high pyrolysis temperatures [24,35].

The N_2 adsorption/desorption isotherms exhibit the type IV isotherm related to physical adsorption, and their loops belong to the H3 type, according to the classification of the International Union of Pure and Applied Chemistry (**Fig. S2**), which indicates the existence of a slit-like mesoporous structure in the char [24,45]. The specific surface area of the char presents an increasing trend with rising temperature (Table 2). Similarly, adding RS has a positive effect on the development of the porosity and specific surface area of the char (25.1 m^2/g for S1R0−600 to 117.2 m^2/g for S3R2−600). Accordingly, the enhancement in char specific surface area causes an increase in the pore volume and a decrease in the average pore diameter. The variations in the porosity of char also verify the changes in surface morphology. In particular, addition of 20 and 40 wt.% of RS can bring remarkable improvement in the BET specific surface area with 2.83 and 5.04 times increases, compared with that of IS, respectively, suggesting better application in wastewater treatment.

3.4. Fourier transform infrared spectra

Among all spectra, many bonded functional groups can be observed in the spectra of raw materials (Fig. 4). The specific stretching vibrations appear at approximately 3600 cm^{-1} (−OH from mineral matter), 3400 cm^{-1} (−OH from hydroxyl or carboxyl), 2950 cm^{-1} (aliphatic −CH asymmetric stretch), 2850 cm^{-1} (aliphatic −CH symmetric stretch), 1625 cm^{-1} (−CONH– and C═O in amide groups and C═C),

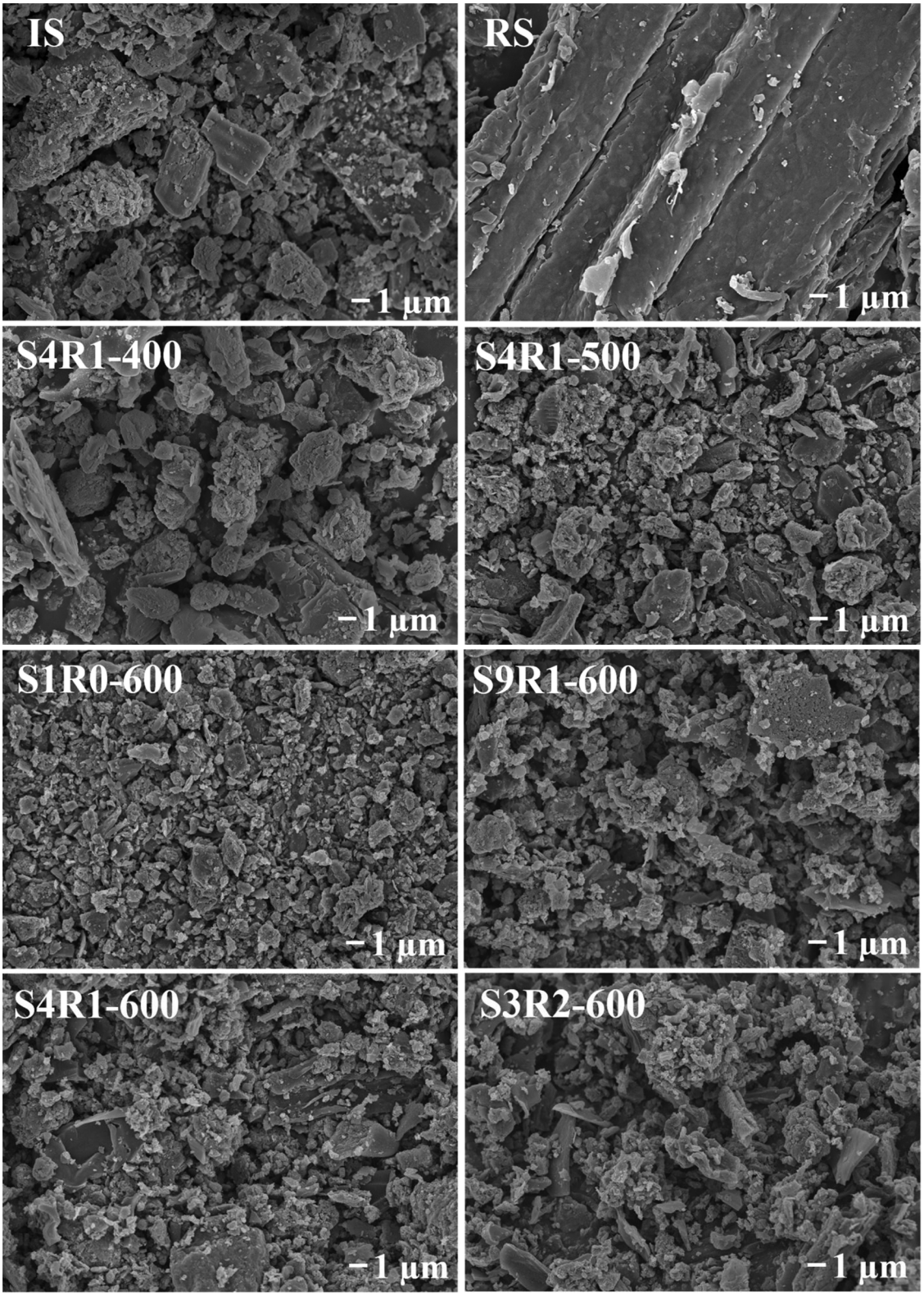

Fig. 3. Surface morphology of feedstocks and char samples.

1050 cm^{-1} (aromatic C—O—C), 800 cm^{-1} (aromatic groups and heteroaromatic compounds), and 400–600 cm^{-1} (metal halogen groups) [16,23,36,45]. RS has stronger stretching vibrations of aliphatic —CH compared with IS spectrum as a result of its large lignocellulose content. The broad peak of amide groups is derived from the presence of protein or amino acid in IS. Moreover, the evident peak at 800 cm^{-1} from IS suggests more metallic groups existed in organic and inorganic halogens compounds, which is the main difference between sludge and other plants materials [44]. After the preparation of char, stretching vibrations remained largely, but the intensities of the surface functional groups become significantly weaker, which is related to the dehydration and decarboxylation reactions [28]. The intensity of the broad

Table 2
Pore properties of industrial sludge and char samples.

Sample	BET specific surface area (m^2/g)	Total pore volume (cm^3/g)	Average pore diameter (nm)
IS	19.4	0.07	14.7
S4R1 – 400	24.8	0.08	13.1
S4R1 – 500	33.5	0.08	9.8
S1R0 – 600	25.1	0.07	11.1
S9R1 – 600	44.8	0.08	7.3
S4R1 – 600	74.3	0.10	5.1
S3R2 – 600	117.2	0.12	4.0

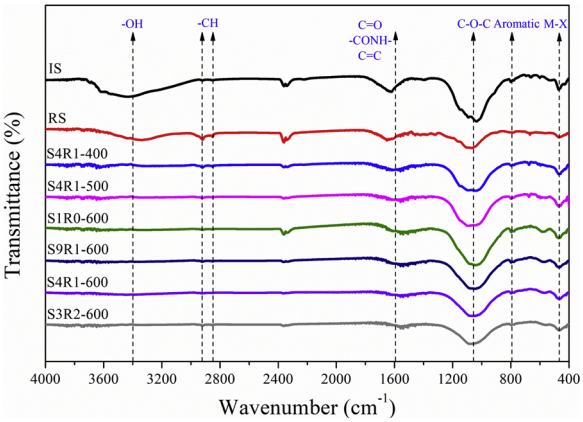

Fig. 4. Fourier transform infrared spectra of feedstocks and char samples.

band from −OH deceasing significantly suggests that a larger amount of free and associated hydroxyl or carboxyl groups are decomposed after pyrolysis. This has been observed in municipal sludge and manure [39,44]. The disappearance of the aliphatic −CH vibration can be attributed to the conversion of organic fatty hydrocarbons into aromatic structures, or CO_2, CH_4, and other gases [21]. The decrease in the −CO−NH− vibration intensity in char verifies the variation of N content and N/C (Table 1). The excursion of the −CO−NH− vibration after co-pyrolysis suggests its complexation with HMs during pyrolysis [46]. The decrease in aromatic C−O−C intensity involves the breakage of the aromatic C−O linkages, volatilization of oxygen in different compounds, and poly-condensation of the aromatic structure [44]. The increase in the intensity of the aromatic groups with increasing temperature suggests that it can provide π electrons and promote strong bonding with the HM cations [7]. Based on the aforementioned discussion, pyrolysis temperature has a greater impact on the surface functional groups compared with the addition of RS and in particular, the catalysis action of high ash content in IS will facilitate the decomposition of these groups [28]. However, the char obtained with abundant C−O−C is beneficial to the removal of organic pollutants in wastewater [47].

3.5. Heavy metals in char

The order of HM concentrations in IS is as follows: Zn > Cr > Cu > Ni > Pb > Cd (**Table S1**). Generally, the concentrations of some HMs in IS from different industries can reach high levels. In the present study, the concentration of Zn in IS is extremely high (> 12,000 mg/kg), whereas the other HM concentrations are lower than 300 mg/kg. This is because large amounts of $ZnSO_4$ are added in the process of the fabrication of fibrous materials. In particular, the Zn concentration has far exceeded the threshold value regulated by the Chinese Standard (GB/T 23485 – 2009: Quality of sludge for co-landfilling) and those reported by municipal sludge [21,35]. However, the concentrations of Cr, Ni, Cu, Cd, and Pb are lower than other IS from electronic and pharmaceutical industries

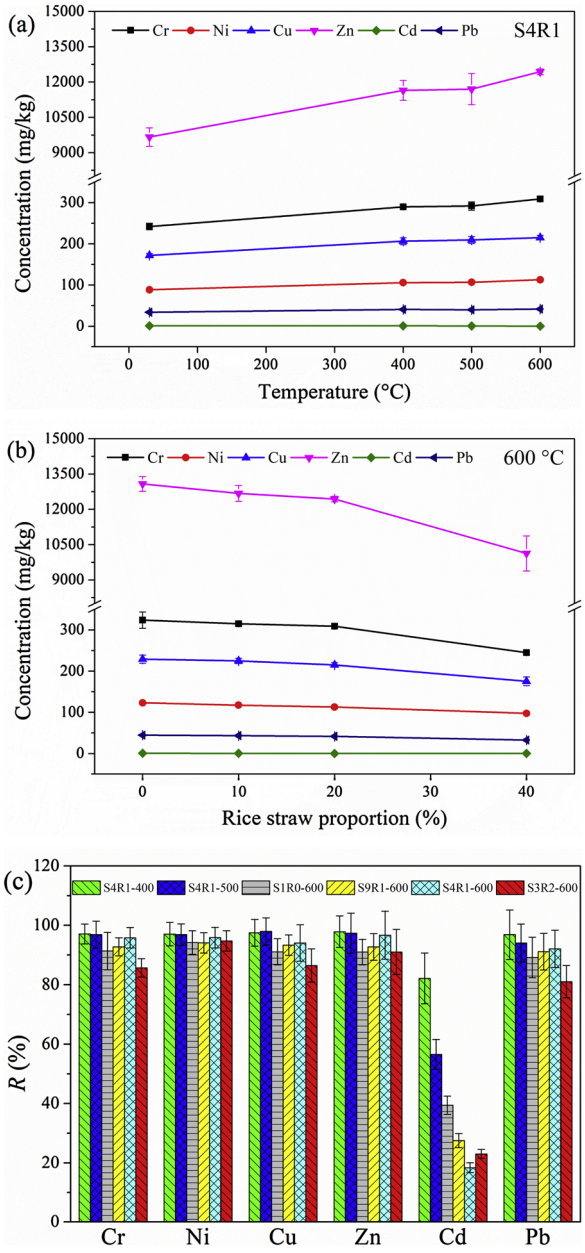

Fig. 5. (a-b) Total concentrations and (c) residual rates of heavy metals in industrial sludge and char samples. a: the samples were obtained at different temperatures for the mixture of industrial sludge and rice straw (4:1, w/w); b: the samples were obtained from different rice straw proportions at 600 °C.

[18,28], and therefore, the direct landfills of this IS will bring potential Zn pollution to the environment. After char preparation, the Cr, Ni, Cu, and Zn concentrations in the samples present an increasing trend with rising temperature (Fig. 5a). These results may be due to the lower losses in the weight of the HMs than those of the organic matter, including large amounts of C, H, and N that result in the enrichment of HMs in the char matrix [7]. Additionally, the concentrations of HMs (except Cd) in char decrease significantly with the increasing ratio of RS addition (Fig. 5b), owing to the dilution effect of RS, including low contents of HMs. Specifically, the Zn concentration in S3R2 – 600 decreases by 22.56 % compared with that of S1R0 – 600. However, Zn concentrations in the char samples obtained after the addition of RS still exceed GB/T 23485 – 2009, and hence, it is important for assessing the speciation distribution and leaching toxicity of HMs.

The residual rates of HMs (except Cd) in char are higher than 80 %

(Fig. 5c), indicating that these HMs mainly remain in the solid product after pyrolysis. However, the residual rate of Cd is below 40 % when the temperature reaches 600 °C. It was reported that Cd bound to carbonate was easily volatilized during pyrolysis, and similar results can be found in textile dyeing sludge [16]. Moreover, a higher pyrolysis temperature decreases the residual rates of HMs in the char owing to the migration of HMs into other phases. Moderate RS addition can promote the retention of HMs (except Cd) in char and decrease the emission of metal vapor through adsorption by the pore structure [18], which has rarely been reported in the study of sludge and biomass. However, a greater RS proportion (S3R2 − 600) would cause a decrease in the residual rates of HMs as a result of the formation of metal chlorides with high content of volatiles [37].

The environmental impact of char samples is directly determined by the speciation distributions of HMs. The F1 and F2 fractions can be adsorbed on the particle surface or combined with carbonates and Fe–Mn hydroxides, demonstrating high biotoxicity in the environment and therefore, they are recognized as bioavailable fractions. The F3 fraction is bound with sulfides or organic matter, and the F4 is occluded in crystalline structures, which is considered a stable fraction [26], and thus, the stability of HM speciation is ranked as follows: F4 > F3 > F2 > F1. Fig. 6 shows the changes in the HM speciation in the IS and char samples. The F3 fractions of Cr, Ni, and Cu in IS have high proportions (35.05 %, 45.82 %, and 37.49 %, respectively), and the F1 + F2 fractions of Zn and Cd reach 55.17 % and 35.88 %, respectively. Similar results were also reported in textile dyeing sludge [16]. However, Pb is primarily distributed to the stable F4 fraction (> 97 %), in agreement with previous research on municipal sludge [7]. These

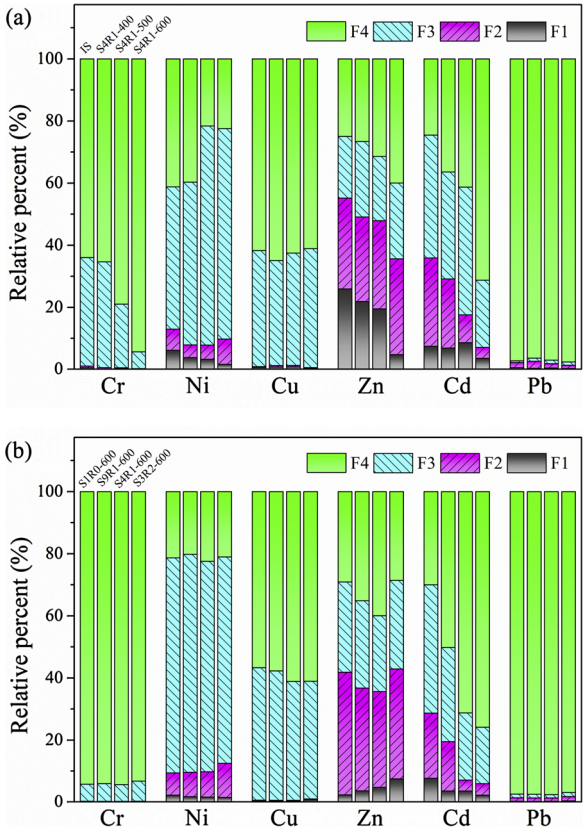

Fig. 6. Speciation distributions of heavy metals in industrial sludge and char samples. a: the samples were obtained at different temperatures; b: the samples were obtained from different rice straw proportions.

results indicate a high potential risk of IS without proper treatment. After char preparation, the F3 fraction of Cr and the F1 + F2 fractions of Zn and Cd decrease substantially with an increase in temperature. Simultaneously, the F4 fractions of Cr, Zn, and Cd exhibit an increasing trend, because unstable HMs in IS are first dissolved and then bound with the crystal lattices to form a more stable state during pyrolysis [48]. The densification of the char after the decomposition of organic matter causes an increase in the F3 fractions of Ni and Cu [18]. Furthermore, the speciation of each HM has different variations after the addition of RS. Specifically, the F1 + F2 fraction of Zn decreases from 41.81 % for S1R0 − 600 to 35.6 % for S4R1 − 600, with the F4 fraction increasing from 29.10% to 39.99%. The F1 + F2 fraction of Cd decreases from 28.67 % to 5.87 % as the RS proportion increases to 40 %. Accordingly, the F4 fraction of Cd increases from 29.99 % to 75.85 %. The F3 fraction of Cu decreases slightly, and the F4 fraction increases after RS addition. These results can be explained due to the released HMs being entrapped by the enlarged structure of biomass, or chelated with some functional groups and inorganic substances [14,49]. While Jin et al. [14] found that bamboo sawdust substantially increased the F4 fractions of Cr and Pb in municipal sludge char, something was not observed in the present study due to high F4 percentage for Cr and Pb in IS. Furthermore, the increases in F1 fraction for Cu and Zn with more RS addition is due to the formation of metal chloride [18], which is different from the effects of other types of biomass (cotton stalks and bamboo sawdust) on HM immobilization [14,50].

3.6. Relationship of heavy metals with char properties

The crystallographic structure of Zn was investigated because of the high concentration of Zn in IS (**Fig. S3**). The main inorganic compounds are SiO_2 and $AlPO_4$ in the feedstock, which is verified in the properties of high ash content in IS [43]. Furthermore, the crystallographic species of Zn are mainly related to the compounds bound with Fe, Mn, and S (Wurtzite-2 H) [18]. The inorganic composition in char exhibits an insignificant change after char preparation, which suggests that the formation of new stable crystal phases is not the main reason for Zn immobilization at the low temperature of 600 °C. The Pearson correlation coefficient can reflect the degree of correlation between the HM speciation and the characteristics of the sample. The larger absolute value indicates a stronger correlation (Fig. 7). The pH shows significant negative correlations with the F1 + F2 fractions of Cr, Zn, Cd, and Pb (Fig. 7a) and positive correlations with the F4 fractions of Cr and Cd (Fig. 7c). However, the increase in pH inhibits the stability of Ni speciation as a result of the significant positive correlation with the F3 fraction (Fig. 7b) and significant negative correlation with the F4 fraction. A similar result was also found in municipal sludge [7]. There is a significant positive correlation with the F4 fraction of Cr for the ash content in char because some oxides and mineral residue related to metals are immobilized in char as ash content [44]. A significant correlation cannot be found between ash content and the F4 fraction of Zn, which has been verified by crystallographic analysis. H/C shows significant positive correlations with the F1 + F2 fractions of Cr, Zn, and Cd and a negative correlation with the F3 fraction of Pb. For the BET specific surface area, there are marked negative correlations with the F1 + F2 fraction and F3 fraction of Cd and a positive correlation with the F4 fraction. Other HM speciations exhibit insignificant correlations with specific surface area as a result of the high residual rates in char. According to this analysis, the promotion of RS on HM immobilization during IS pyrolysis can be summarized as follows: (1) RS can decrease the dissolution of HM by increasing the alkalinity of char, (2) the formation of an aromatic structure has a positive influence on HM stability, and (3) the greater specific surface area allows better contact

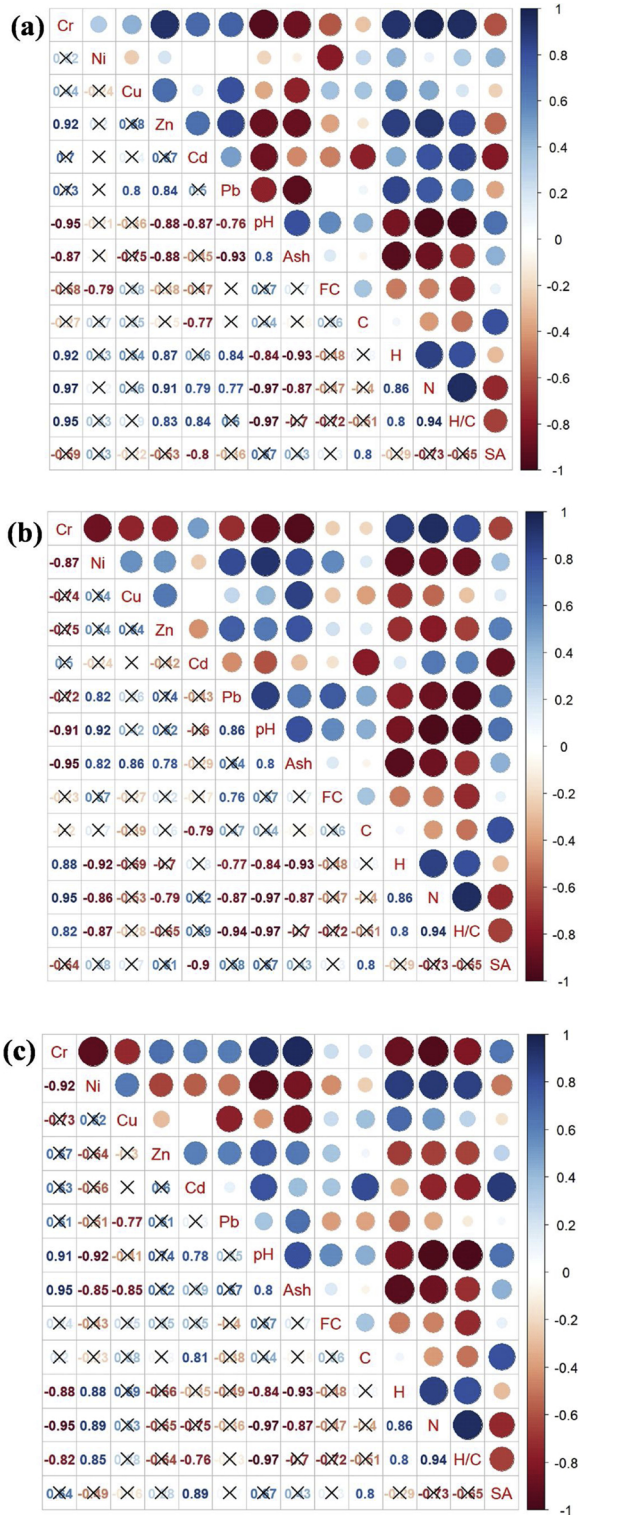

Fig. 7. Pearson correlation between heavy metal speciation and characteristics of industrial sludge and char samples: (a) F1 + F2 fractions; (b) F3 fraction; (c) F4 fraction. The color (red to blue) indicates the change in correlation from negative to positive and the size of bubble shows the strength of correlation, which can be expressed by skew-symmetric numbers. Cross shows non-significant correlation between heavy metal and char property ($P > 0.05$). SA presents BET specific surface area.

between the liquid and solid particle and can decrease the leaching of HMs after the addition of RS [15,18,37].

3.7. Risk assessment of char

The leaching concentration of Zn in IS is extremely high (152.228 mg/L), exceeding the threshold value from the Chinese National Standard (GB-5085.3–2007), listed in Table 3. This suggests that IS would be restricted for application in the environment. The leaching concentrations of Cr, Ni, and Zn in char substantially decrease after char preparation, and moderate RS addition (< 40 %) can further reduce the leaching toxicity of these HMs. The increase in Cu leaching efficiency for char obtained at 400–500 °C can be attributed to the formation of metal chloride [18]. In addition, the leaching concentrations of Cd and Pb have extremely low levels (< 0.01 mg/L). In particular, S4R1 − 600 has the lowest leaching toxicity of HMs and satisfies the requirements of GB-5085.3–2007, which suggests that this improved char can be applied safely in the construction and adsorption field.

The environmental influence of HMs in char derived from the co-pyrolysis of IS with RS can be analyzed through potential ecological risk assessment, which is determined by the summation of the risk indices of HMs [16]. The C_f values of Zn and Cd in IS reach 3.01 and 3.08, respectively, indicating their moderate contamination levels (Fig. 8). The C_f value of Ni in IS is 1.43, suggesting a low contamination level. The C_f values of the other HMs have negligible contamination levels (lower than 1.0) and furthermore, the E_r value of Cd (92.35) in IS indicates its considerable ecological level. The *RI* of IS reaches 108.28, contributed mainly by Cd (85.29 %) and has a considerable contamination level. After the preparation of char, the C_f and E_r values of Cr, Zn, and Cd decrease significantly, and the addition of RS can further reduce the potential ecological level of HMs. However, the E_r value of Ni presents an increasing trend after pyrolysis, although still at a low ecological level. These results are in accordance with those of the HM speciation. Simultaneously, the *RI* values of HMs in char decrease markedly with increasing pyrolysis temperature and moderate RS proportion. The *RI* of the HMs in S4R1 − 600 exhibits the lowest value of 37.75, with a low contamination level.

4. Conclusions

This study was conducted for the treatment of IS with high ash and HM contents by co-pyrolysis with RS. After co-pyrolysis, the ash content is decreased and the thermal stability, aromaticity, and pore structure of char are increased, due to the high organic contents in RS. In addition, the reduction in HM concentrations in char was observed after the addition of RS due to the dilution effect. Moderate addition of RS can promote the retention of HMs in char and decrease the emission of metal vapor. A higher pyrolysis temperature and suitable RS proportion can also promote the transformation of Cr, Zn, and Cd from the bioavailable states to more stable forms, because of the higher alkalinity, aromaticity, and specific surface area of char. In summary, 600 °C and an RS addition of 20 % are the optimal conditions, and the obtained char has better application potential, with low leaching toxicity and potential ecological risk of HM.

CRediT authorship contribution statement

Shengyu Xie: Conceptualization, Data curation, Formal analysis, Visualization, Writing - original draft. **Guangwei Yu:** Conceptualization, Writing - review & editing, Project administration, Supervision. **Chunxing Li:** Writing - review & editing. **Jie Li:** Writing -

Table 3
Leaching concentrations of heavy metals in industrial sludge and char samples.

Sample	Leaching concentration (mg/L)					
	Cr	Ni	Cu	Zn	Cd	Pb
IS	0.027 ± 0.001	0.221 ± 0.003	0.018 ± 0.001	152.228 ± 4.804	0.002 ± 0.000	0.004 ± 0.000
S4R1 − 400	0.007 ± 0.000	0.118 ± 0.007	0.030 ± 0.001	97.221 ± 4.947	0.002 ± 0.000	0.006 ± 0.000
S4R1 − 500	0.007 ± 0.000	0.094 ± 0.006	0.035 ± 0.002	104.175 ± 3.898	0.001 ± 0.000	0.005 ± 0.000
S1R0 − 600	0.006 ± 0.001	0.180 ± 0.008	0.021 ± 0.005	107.737 ± 2.861	*ND*[b]	0.005 ± 0.000
S9R1 − 600	0.005 ± 0.000	0.097 ± 0.008	0.023 ± 0.002	46.787 ± 0.511	*ND*	0.003 ± 0.000
S4R1 − 600	0.004 ± 0.001	0.057 ± 0.002	0.016 ± 0.002	23.824 ± 1.228	*ND*	0.003 ± 0.000
S3R2 − 600	0.007 ± 0.000	0.099 ± 0.007	0.032 ± 0.001	53.323 ± 4.636	*ND*	0.003 ± 0.000
Standard[a]	15	5	100	100	1	5

[a] Identification standard for standards for hazardous wastes from China (GB-5085.3–2007).
[b] *ND*, not detected.

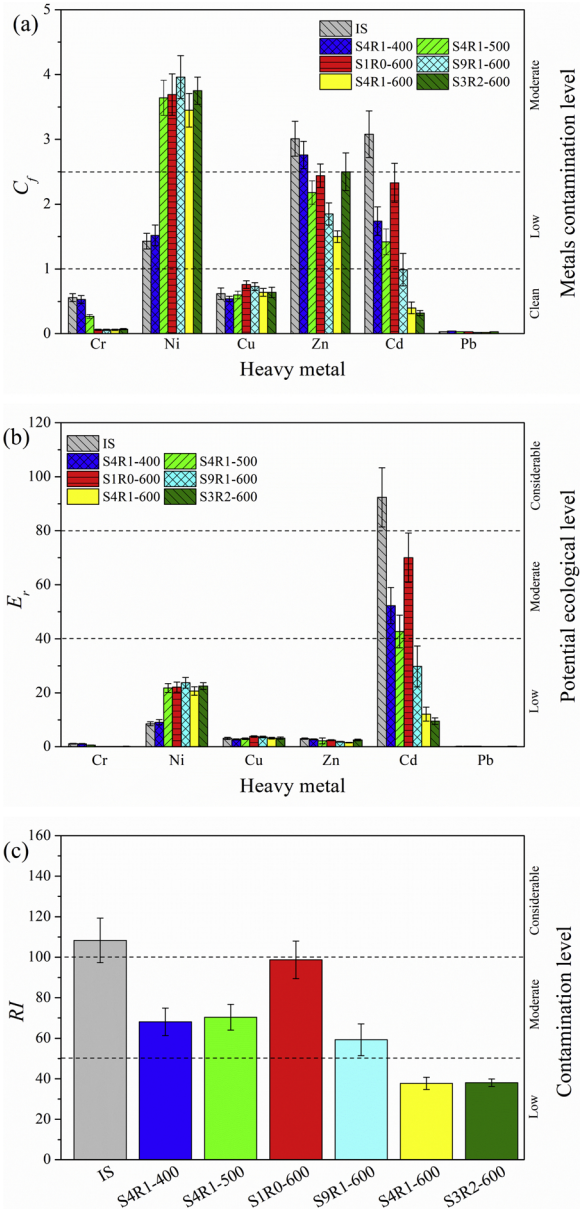

Fig. 8. (a) C_f, (b) E_r, and (c) *RI* indices of heavy metals in industrial sludge and char samples.

review & editing. **Gang Wang:** Data curation. **Shaoqing Dai:** Visualization. **Yin Wang:** Project administration, Supervision.

Declaration of Competing Interest

The authors declare that they have no known competing financial interests or personal relationships that could have appeared to influence the work reported in this paper.

Acknowledgments

This work was supported by the Strategic Priority Research Program of the Chinese Academy of Sciences [XDA23020504, XDA23030301], Natural Science Foundation of Fujian Province [2019J01135], Science and Technology Program of Xiamen [3502Z20193076], and Industry Leading Key Projects of Fujian Province [2015H0044].

Appendix A. Supplementary data

Supplementary material related to this article can be found, in the online version, at doi:https://doi.org/10.1016/j.jaap.2020.104866.

References

[1] M.S. Islam, M.K. Ahmed, M. Raknuzzaman, M. Habibullah-Al-Mamun, G.K. Kundu, Heavy metals in the industrial sludge and their ecological risk: a case study for a developing country, J. Geochem. Explor. 172 (2017) 41–49, https://doi.org/10.1016/j.gexplo.2016.09.006.
[2] R. Ma, S. Sun, H. Geng, L. Fang, P. Zhang, X. Zhang, Study on the characteristics of microwave pyrolysis of high-ash sludge, including the products, yields, and energy recovery efficiencies, Energy 144 (2018) 515–525, https://doi.org/10.1016/j.energy.2017.12.085.
[3] M. Naseri, A. Vazirzadeh, R. Kazemi, F. Zaheri, Concentration of some heavy metals in rice types available in Shiraz market and human health risk assessment, Food Chem. 175 (2015) 243–248, https://doi.org/10.1016/j.foodchem.2014.11.109.
[4] J. Peccia, P. Westerhoff, We should expect more out of our sewage sludge, Environ. Sci. Technol. 49 (2015) 8271–8276, https://doi.org/10.1021/acs.est.5b01931.
[5] H. Chen, S.H. Yan, Z.L. Ye, H.J. Meng, Y.G. Zhu, Utilization of urban sewage sludge: Chinese perspectives, Environ. Sci. Pollut. R. 19 (2012) 1454–1463, https://doi.org/10.1007/s11356-012-0760-0.
[6] D. Chen, L. Yin, H. Wang, P. He, Pyrolysis technologies for municipal solid waste: a review, Waste Manage. 34 (2014) 2466–2486, https://doi.org/10.1016/j.wasman.2014.08.004.
[7] X. Wang, Q. Chi, X. Liu, Y. Wang, Influence of pyrolysis temperature on characteristics and environmental risk of heavy metals in pyrolyzed biochar made from hydrothermally treated sewage sludge, Chemosphere 216 (2019) 698–706, https://doi.org/10.1016/j.chemosphere.2018.10.189.
[8] Y. Tang, M.S. Alam, K.O. Konhauser, D.S. Alessi, S. Xu, W. Tian, Y. Liu, Influence of pyrolysis temperature on production of digested sludge biochar and its application for ammonium removal from municipal wastewater, J. Cleaner Prod. 209 (2019) 927–936, https://doi.org/10.1016/j.jclepro.2018.10.268.
[9] S. Khan, C. Chao, M. Waqas, H.P.H. Arp, Y.G. Zhu, Sewage sludge biochar influence

upon rice (Oryza sativa L) yield, metal bioaccumulation and greenhouse gas emissions from acidic paddy soil, Environ. Sci. Technol. 47 (2013) 8624–8632, https://doi.org/10.1021/es400554x.
[10] Q. Chen, H. Liu, J. Ko, H. Wu, Q. Xu, Structure characteristics of bio-char generated from co-pyrolysis of wooden waste and wet municipal sewage sludge, Fuel Process. Technol. 183 (2019) 48–54, https://doi.org/10.1016/j.fuproc.2018.11.005.
[11] Y. Zhou, Y. Liu, W. Jiang, L. Shao, L. Zhang, L. Feng, Effects of pyrolysis temperature and addition proportions of corncob on the distribution of products and potential energy recovery during the preparation of sludge activated carbon, Chemosphere 221 (2019) 175–183, https://doi.org/10.1016/j.chemosphere.2019.01.026.
[12] T. Wang, Y. Chen, J. Li, Y. Xue, J. Liu, M. Mei, H. Hou, S. Chen, Co-pyrolysis behavior of sewage sludge and rice husk by TG-MS and residue analysis, J. Cleaner Prod. 250 (2020) 119557, , https://doi.org/10.1016/j.jclepro.2019.119557.
[13] Q. Yin, M. Liu, H. Ren, Biochar produced from the co-pyrolysis of sewage sludge and walnut shell for ammonium and phosphate adsorption from water, J. Environ. Manage. 249 (2019) 109410, , https://doi.org/10.1016/j.jenvman.2019.109410.
[14] J. Jin, M. Wang, Y. Cao, S. Wu, P. Liang, Y. Li, J. Zhang, J. Zhang, M.H. Wong, S. Shan, P. Christie, Cumulative effects of bamboo sawdust addition on pyrolysis of sewage sludge: biochar properties and environmental risk from metals, Bioresour. Technol. 228 (2017) 218–226, https://doi.org/10.1016/j.biortech.2016.12.103.
[15] P. Devi, A.K. Saroha, Risk analysis of pyrolyzed biochar made from paper mill effluent treatment plant sludge for bioavailability and eco-toxicity of heavy metals, Bioresour. Technol. 162 (2014) 308–315, https://doi.org/10.1016/j.biortech.2014.03.093.
[16] X. Wang, C. Li, Z. Li, G. Yu, Y. Wang, Effect of pyrolysis temperature on characteristics, chemical speciation and risk evaluation of heavy metals in biochar derived from textile dyeing sludge, Ecotoxicol. Environ. Saf. 168 (2019) 45–52, https://doi.org/10.1016/j.ecoenv.2018.10.022.
[17] R. Jothiramalingam, S.L. Lo, Cl. Chen, Effects of different additives with assistance of microwave heating for heavy metal stabilization in electronic industry sludge, Chemosphere 78 (2010) 609–613, https://doi.org/10.1016/j.chemosphere.2009.10.065.
[18] W.D. Chanaka Udayanga, A. Veksha, A. Giannis, Y.N. Liang, G. Lisak, X. Hu, T.-T. Lim, Insights into the speciation of heavy metals during pyrolysis of industrial sludge, Sci. Total Environ. 691 (2019) 232–242, https://doi.org/10.1016/j.scitotenv.2019.07.095.
[19] D. Chen, Q. Ma, L. Wei, N. Li, Q. Shen, W. Tian, J. Zhou, J. Long, Catalytic hydroliquefaction of rice straw for bio-oil production using Ni/CeO2 catalysts, J. Anal. Appl. Pyrolysis 130 (2018) 169–180, https://doi.org/10.1016/j.jaap.2018.01.012.
[20] Y.F. Huang, C.H. Shih, P.T. Chiueh, S.L. Lo, Microwave co-pyrolysis of sewage sludge and rice straw, Energy 87 (2015) 638–644, https://doi.org/10.1016/j.energy.2015.05.039.
[21] H.J. Huang, T. Yang, F.Y. Lai, G.Q. Wu, Co-pyrolysis of sewage sludge and sawdust/rice straw for the production of biochar, J. Anal. Appl. Pyrolysis 125 (2017) 61–68, https://doi.org/10.1016/j.jaap.2017.04.018.
[22] Sq. Zhang, Xm. Yue, Zy. Yin, Tt. Pan, Mj. Dong, Ty. Sun, Study of the co-pyrolysis behavior of sewage-sludge/rice-straw and the kinetics, Procedia Earth Planet. Sci 1 (2009) 661–666, https://doi.org/10.1016/j.proeps.2009.09.104.
[23] J. Li, G. Yu, L. Pan, C. Li, F. You, S. Xie, Y. Wang, J. Ma, X. Shang, Study of ciprofloxacin removal by biochar obtained from used tea leaves, J. Environ. Sci. 73 (2018), https://doi.org/10.1016/j.jes.2017.12.024.
[24] A. Zielińska, P. Oleszczuk, B. Charmas, J. Skubiszewska-Zięba, S. Pasieczna-Patkowska, Effect of sewage sludge properties on the biochar characteristic, J. Anal. Appl. Pyrolysis 112 (2015) 201–213, https://doi.org/10.1016/j.jaap.2015.01.025.
[25] R. Wallace, M. Seredych, P. Zhang, T.J. Bandosz, Municipal waste conversion to hydrogen sulfide adsorbents: investigation of the synergistic effects of sewage sludge/fish waste mixture, Chem. Eng. J. 237 (2014) 88–94, https://doi.org/10.1016/j.cej.2013.10.005.
[26] S. Xie, G. Yu, C. Li, F. You, J. Li, R. Tian, G. Wang, Y. Wang, Dewaterability enhancement and heavy metals immobilization by pig manure biochar addition during hydrothermal treatment of sewage sludge, Environ. Sci. Pollut. R. 26 (2019) 16537–16547, https://doi.org/10.1007/s11356-019-04961-1.
[27] T. Li, F. Guo, X. Li, Y. Liu, K. Peng, X. Jiang, C. Guo, Characterization of herb residue and high ash-containing paper sludge blends from fixed bed pyrolysis, Waste Manage. 76 (2018) 544–554, https://doi.org/10.1016/j.wasman.2018.04.002.
[28] W.D. Chanaka Udayanga, A. Veksha, A. Giannis, T.-T. Lim, Pyrolysis derived char from municipal and industrial sludge: impact of organic decomposition and inorganic accumulation on the fuel characteristics of char, Waste Manage. 83 (2019) 131–141, https://doi.org/10.1016/j.wasman.2018.11.008.
[29] W. Zuo, B. Jin, Y. Huang, Z. Xie, Investigation of waste metalworking fluids sludge pyrolysis for characterization of pyrolysis oil and char properties, J. Anal. Appl. Pyrolysis 116 (2015) 168–176, https://doi.org/10.1016/j.jaap.2015.09.013.
[30] S. Fang, Z. Yu, Y. Lin, S. Hu, Y. Liao, X. Ma, Thermogravimetric analysis of the co-pyrolysis of paper sludge and municipal solid waste, Energy Convers. Manage. 101 (2015) 626–631, https://doi.org/10.1016/j.enconman.2015.06.026.
[31] S. Zhao, M. Liu, L. Zhao, L. Zhu, Influence of interactions among three biomass components on the pyrolysis behavior, Ind. Eng. Chem. Res. 57 (2018) 5241–5249, https://doi.org/10.1021/acs.iecr.8b00593.
[32] X. Peng, X. Ma, Y. Lin, Z. Guo, S. Hu, X. Ning, Y. Cao, Y. Zhang, Co-pyrolysis between microalgae and textile dyeing sludge by TG–FTIR: kinetics and products, Energy Convers. Manage. 100 (2015) 391–402, https://doi.org/10.1016/j.enconman.2015.05.025.
[33] J. Li, G. Yu, L. Pan, C. Li, F. You, Y. Wang, Ciprofloxacin adsorption by biochar derived from co-pyrolysis of sewage sludge and bamboo waste, Environ. Sci. Pollut. R. (2020), https://doi.org/10.1007/s11356-020-08333-y.
[34] T. Chen, Y. Zhang, H. Wang, W. Lu, Z. Zhou, Y. Zhang, L. Ren, Influence of pyrolysis temperature on characteristics and heavy metal adsorptive performance of biochar derived from municipal sewage sludge, Bioresour. Technol. 164 (2014) 47–54, https://doi.org/10.1016/j.biortech.2014.04.048.
[35] Z. Wang, K. Liu, L. Xie, H. Zhu, S. Ji, X. Shu, Effects of residence time on characteristics of biochars prepared via co-pyrolysis of sewage sludge and cotton stalks, J. Anal. Appl. Pyrolysis (2019) 104659, , https://doi.org/10.1016/j.jaap.2019.104659.
[36] Z. Ma, Y. Yang, Q. Ma, H. Zhou, X. Luo, X. Liu, S. Wang, Evolution of the chemical composition, functional group, pore structure and crystallographic structure of biochar from palm kernel shell pyrolysis under different temperatures, J. Anal. Appl. Pyrolysis 127 (2017) 350–359, https://doi.org/10.1016/j.jaap.2017.07.015.
[37] Y. Xu, F. Qi, T. Bai, Y. Yan, C. Wu, Z. An, S. Luo, Z. Huang, P. Xie, A further inquiry into co-pyrolysis of straws with manures for heavy metal immobilization in manure-derived biochars, J. Hazard. Mater. 380 (2019) 120870, , https://doi.org/10.1016/j.jhazmat.2019.120870.
[38] P. Zhang, X. Zhang, Y. Li, L. Han, Influence of pyrolysis temperature on chemical speciation, leaching ability, and environmental risk of heavy metals in biochar derived from cow manure, Bioresour. Technol. 302 (2020) 122850, , https://doi.org/10.1016/j.biortech.2020.122850.
[39] R. Tian, C. Li, S. Xie, F. You, Z. Cao, Z. Xu, G. Yu, Y. Wang, Preparation of biochar via pyrolysis at laboratory and pilot scales to remove antibiotics and immobilize heavy metals in livestock feces, J. Soils Sediments 19 (2019) 2891–2902, https://doi.org/10.1007/s11368-019-02350-2.
[40] J. Liu, S. Huang, K. Chen, T. Wang, M. Mei, J. Li, Preparation of biochar from food waste digestate: Pyrolysis behavior and product properties, Bioresour. Technol. 302 (2020) 122841, , https://doi.org/10.1016/j.biortech.2020.122841.
[41] R. Al Afif, S.S. Anayah, C. Pfeifer, Batch pyrolysis of cotton stalks for evaluation of biochar energy potential, Renew. Energ. 147 (2020) 2250–2258, https://doi.org/10.1016/j.renene.2019.09.146.
[42] S. Yu, J. Park, M. Kim, C. Ryu, J. Park, Characterization of biochar and byproducts from slow pyrolysis of hinoki cypress, Bioresour. Technol. Rep. 6 (2019) 217–222, https://doi.org/10.1016/j.biteb.2019.03.009.
[43] J. Li, G. Yu, S. Xie, L. Pan, C. Li, F. You, Y. Wang, Immobilization of heavy metals in ceramsite produced from sewage sludge biochar, Sci. Total Environ. 628-629 (2018) 131–140, https://doi.org/10.1016/j.scitotenv.2018.02.036.
[44] J. Jin, Y. Li, J. Zhang, S. Wu, Y. Cao, P. Liang, J. Zhang, M.H. Wong, M. Wang, S. Shan, P. Christie, Influence of pyrolysis temperature on properties and environmental safety of heavy metals in biochars derived from municipal sewage sludge, J. Hazard. Mater. 320 (2016) 417–426, https://doi.org/10.1016/j.jhazmat.2016.08.050.
[45] C. Li, J. Li, L. Pan, X. Zhu, S. Xie, G. Yu, Y. Wang, X. Pan, G. Zhu, I. Angelidaki, Treatment of digestate residues for energy recovery and biochar production: From lab to pilot-scale verification, J. Cleaner Prod. 265 (2020) 121852, , https://doi.org/10.1016/j.jclepro.2020.121852.
[46] H. Lu, W. Zhang, S. Wang, L. Zhuang, Y. Yang, R. Qiu, Characterization of sewage sludge-derived biochars from different feedstocks and pyrolysis temperatures, J. Anal. Appl. Pyrolysis 102 (2013) 137–143, https://doi.org/10.1016/j.jaap.2013.03.004.
[47] C.P. Silva, G. Jaria, M. Otero, V.I. Esteves, V. Calisto, Adsorption of pharmaceuticals from biologically treated municipal wastewater using paper mill sludge-based activated carbon, Environ. Sci. Pollut. R. 26 (2019) 13173–13184, https://doi.org/10.1007/s11356-019-04823-w.
[48] H. Yuan, T. Lu, H. Huang, D. Zhao, N. Kobayashi, Y. Chen, Influence of pyrolysis temperature on physical and chemical properties of biochar made from sewage sludge, J. Anal. Appl. Pyrolysis 112 (2015) 284–289, https://doi.org/10.1016/j.jaap.2015.01.010.
[49] W. Shi, C. Liu, Y. Shu, C. Feng, Z. Lei, Z. Zhang, Synergistic effect of rice husk addition on hydrothermal treatment of sewage sludge: fate and environmental risk of heavy metals, Bioresour. Technol. 149 (2013) 496–502, https://doi.org/10.1016/j.biortech.2013.09.114.
[50] Z. Wang, L. Xie, K. Liu, J. Wang, H. Zhu, Q. Song, X. Shu, Co-pyrolysis of sewage sludge and cotton stalks, Waste Manage. 89 (2019) 430–438, https://doi.org/10.1016/j.wasman.2019.04.033.